GPS/IRS hybridization : definition of exclusion radius using solution separation method

Anne-Christine Escher, Christophe Macabiau, Benoit Roturier, Nicolas Martin

Escher A.C., Ecole Nationale de l'Aviation Civile, France
Macabiau C., Ecole Nationale de l'Aviation Civile, France
Roturier B., Service Technique de la Navigation Aerienne, France
Martin N., Thales Avionics, France

GPS/IRS HYBRIDIZATION: DEFINITION OF EXCLUSION RADIUS USING SOLUTION SEPARATION METHOD

ABSTRACT

When hybridizing GPS with IRS, the integrity of GPS signals has to be checked so that slowly growing errors on GPS measurements don't affect inertial calibration.

Several solutions exist to perform fault detection and exclusion of GPS signal.
Some of these depend only on GNSS information but the capacity of RAIM (Receiver Autonomous Integrity Monitoring) is limited. This algorithm greatly depends on the constellation geometry (at least 5 SV are needed for detection) and doesn't have sufficient availability for stringent phases of flight. AAIM (Aircraft Autonomous Integrity Monitoring) algorithms are taking into account additional onboard information such as IRS. The Solution Separation method can be implemented for RAIM or AAIM.

The aim of this paper is to describe the technique inspired from Solution Separation used to compute isolation radius in addition to the classical detection protection level, and to present some simulation results we obtain by implementing this algorithm in a tightly coupled Kalman.

After reviewing civil aviation requirements and defining the tightly coupled Kalman filter that was used, the detection and isolation satellite failure method is described. This method is inspired from the Solution Separation method which is generalised to N subsets of N-1 Kalman filters used to define the isolation radius as presented in [2].
Finally simulated results of the algorithm for NPA are shown.

INTRODUCTION

Tight integration of GPS and inertial information allows enhancing GNSS satellite FDE (fault detection and exclusion) and continuity performance (calibrated IRS may be used for coasting when GNSS information is unavailable).
Solution Separation method has first been introduced by Brenner in 1995 [1]. Assuming that only one failure may occur at a time, fault detection is performed by estimating the separation between the solution given by a main filter and solution from different sub-filters that each exclude measurement from one satellite. This separation is an estimate of the impact of the satellite failure on the IRS position error correction using GPS measurements.
The FDE method presented in this paper is an extension of Brenner's solution separation as it has been defined in [2]. By introducing one more rank of sub-sub-filters (each one is excluding measurement from 2 satellites) the algorithm succeeds in isolating the faulty satellite and proposes a computation of exclusion level.
The aim of this paper is to present some simulation results obtained by implementing the FDE algorithm with false alarm rate and missed detection probability corresponding to NPA phase of flight.
A point is first made on civil aviation assumptions concerning tightly integrated GPS/inertial systems. The FDE process is described and the method for computing protection level is defined. Finally simulated test results are presented.

CIVIL AVIATION ASSUMPTIONS

FDE requirements

Appendix R to RTCA/DO 229C [3] clarifies FDE requirements to GPS/IRS application for en-route to non-precision approach. (Table 1)

Missed detection probability	0.001
False detection rate (SA off)	1/3 10^{-6}/hr
Probability (p_{MI}) of exceeding HPL	10^{-7}/hr
Rare normal performance rate	$<10^{-7}$/sample
Failed exclusion probability	0.001
Continuity	1/3 10^{-6}/hr

Table 1. FDE requirements.

The rare normal performance rate is the probability that the horizontal error exceeds the horizontal alert limit in a fault free case ie in the case of noise only. In case of SA off its value is 10^{-7}/sample. Demonstration in [3] shows that the contribution of the rare normal performance limit HPL_0 which depends on this probability is essential in integrated systems. In the system configuration presented here HPL_0 is the rare normal performance limit of the primary Kalman filter.

FDE performance parameters

Nominal fault detection performance involves three parameters (test metric, decision threshold and protection level PL). The test metric is an observed quantity that is compared to a decision threshold. The decision threshold is chosen on the basis of statistical characteristics of the test metric so that false alert doesn't occur more than a false alert rate P_{FA}. This rate is defined for each phase of flight and depends on the continuity requirement (continuity loss-of-function per hour or phase duration) imposed by ICAO and the GNSS measurements time correlation.

The protection level (HPL/VPL) is the position error that the FDE algorithm guarantees will not be exceeded without being detected by the fault detection function. It depends on the values of missed detection probability P_{MD} and P_{FA}.

As it will be described in the next paragraph, exclusion of the faulty satellite is performed by examining each subset of $N-1$ satellites (where N is the numerous of tracked satellites) and searches the subset without a fault detection condition. Therefore fault exclusion performance involves some similar parameters: a test statistics, decision threshold and exclusion level. The exclusion level is a radius in the horizontal/vertical (HEL/VEL) plane that guarantees that any errors on or beyond this radius due to a satellite failure will be eliminated because of the exclusion function. It is given as the largest PL of the subsets of $N-1$ satellites computed in function of failed exclusion probability P_{FE} and P_{FA}.

SOLUTION SEPARATION METHOD

Fault Detection

Fault Detection algorithm consists in maintaining a primary Kalman filter which incorporates the N measurements of the whole satellite constellation, and as many Kalman sub-filters as the number of satellites (i.e. N sub-filters). The primary filter F_{00} provides IRS correction. Sub-filters which each of these incorporate the measurements from N-1 satellites are dedicated to detection only. They are noted F_{0n}, $n=1\ldots N$. Figure 1.

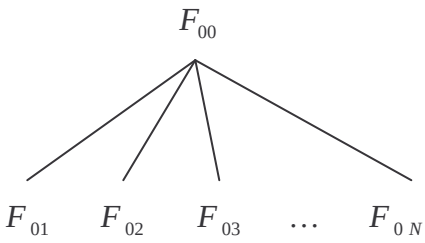

Figure 1. Detection filters hierarchy.

Solution separation between F_{00} and each F_{0n} is estimated: it is the difference in the horizontal/vertical plane between the state vector estimated by F_{00} and the state vector estimated by F_{0n}.

Fault detection is performed by monitoring the separation between the main-solution and each of sub-solutions and comparing it to a computed detection threshold that depends on the separation statistics and P_{FA}. When a failure occurs at least one solution separation will exceed this threshold. This method also guarantees a protection radius against any failure (even

slow ramp) in straight relationship with the threshold and the value of the required P_{MD}.

Fault Exclusion

It assumes that there is only one satellite failure at a time.
In order to perform exclusion for each sub-filter N-1 sub-sub-filters are also maintained. Each of these is excluding the measurement excluded by its "parent" sub-filter, and the measurement from a different satellite. These sub-sub-filters are noted $F_{nm}, n = 1 \ldots N, m = 1 \ldots N, n \neq m.$ Figure 2.

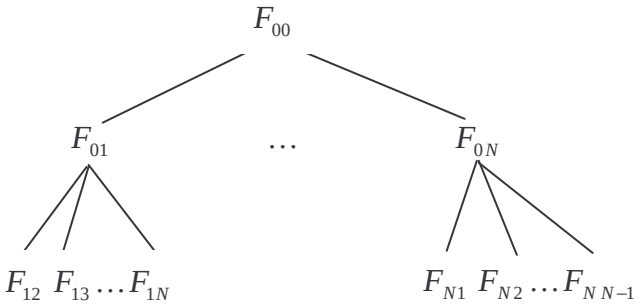

Figure 2. Exclusion filters hierarchy.

When there is a detection, the separation between each sub-sub-filter and its parent sub-filter is computed and compared to an exclusion threshold that depends on the expected separation statistics and P_{FA}. If for sub-filter F_{0n}, there exists one solution separation such that one separation between it and sub-sub-filter F_{nm} exceeds the threshold, it can't be the faulty satellite. But if there is only one sub-filter F_{0n} for which all separations between its solution and its sub-sub-filters F_{nm} are under the threshold, satellite n is the faulty satellite.

GPS/IRS KALMAN HYBRIDIZING FILTERS

All of the Kalman filters are running in the same way.
For any of them, the implemented system is composed of three units: an inertial unit (Inertial measurement Unit + Inertial Reference System), a GNSS receiver (GPS measurements) and an integration process (Kalman filters) that also performed FDE function. Figure 3.

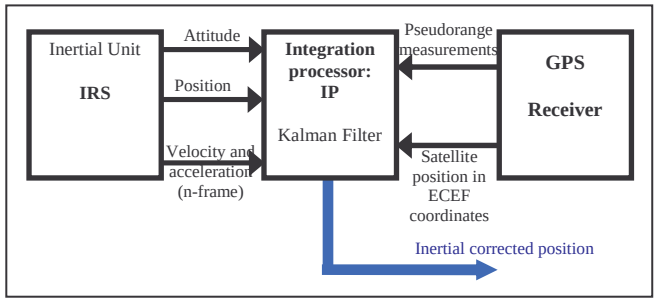

Figure 3. GPS/IRS architecture

All measurements and simulations have been made with Matlab.

Inertial unit

It provides to the integration process Matlab-generated inertial position, velocity and attitude angles and gyrometric and accelerometric measurements.

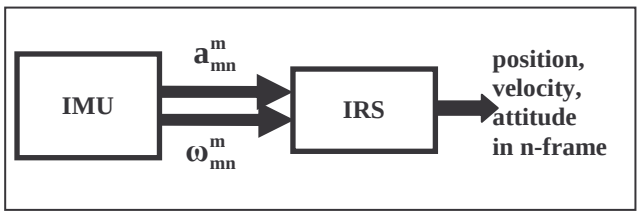

Figure 4. Inertial Unit

Inertial Measurement Unit: IMU

This unit generates realistic gyro and accelero measurements at $100\ Hz$ rate from the data of an aircraft trajectory and attitude angles evolution. These measurements are respectively:

$\mathbf{a}^{m}_{m/i}$ non-gravitational acceleration of the mobile relative to the inertial (absolute) frame in the mobile frame

$\boldsymbol{\omega}^{m}_{m/I}$ angular rate of the mobile relative to the inertial frame in the mobile frame

Sensor noises and biases are also modelled in order to simulate different inertial sensors quality.

Inertial Reference System: IRS

IMU measurements are processed by Strapdown inertial navigation to provide inertial solution at $100\ Hz$. The navigation function gives the mobile positions and velocities relative to the earth frame in the navigation frame. Strapdown inertial navigation scheme is described in figure 5

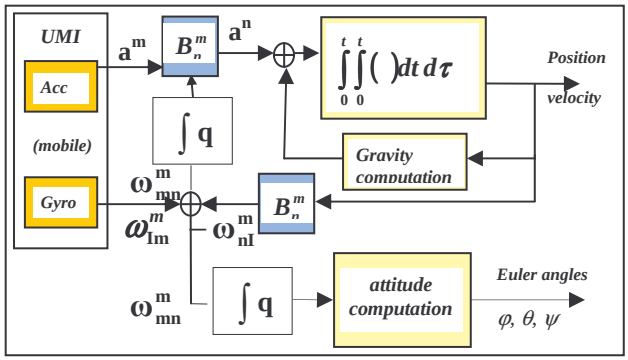

Figure 5. IRS platform computations

$\mathbf{B}_{\mathbf{n}}^{\mathbf{m}}$ is the coordinate transformation matrix that rotates the mobile body frame (m) acceleration measurements to the local north, east and down navigation frame (n). Its components are computed from the integration of gyro measurements.
The attitude determination function determines $\mathbf{B}_{\mathbf{n}}^{\mathbf{m}}$ and the attitude of the mobile body frame to the navigation frame that is to say Euler angles, where φ,θ,ψ stand for roll, pitch, yaw respectively. They are the rotation angles that allow passing from the $m-$frame to the $n-$frame.

Attitude determination method

The attitude algorithm used is the quaternion method ($\int \mathbf{q}$) which offers better numerical and stable characteristics than Euler or Direct Cosine methods.[4]
The single rotation that allows transformation from the $m-$frame to the $n-$frame is represented by the quaternion $\mathbf{q}$. It evolves in accordance with a simple differential equation that is solved using Edwards' method. See [4]

GPS Receiver

Pseudo range measurements (PRs) are generated at $1Hz$. Random noise is added on each satellite measurement and is composed of a correlated noise due to inospheric delay (b_{iono}) and white-Gaussian noise due to noise process (b_{PR}).

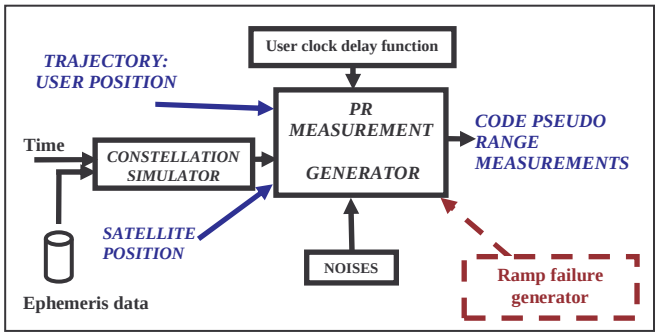

Figure 6. GPS measurements generator

GPS/IRS Kalman filtering system

As shown in figure 3, the output position of the whole system is the corrected inertial position. The role of Kalman filters is to estimate inertial errors using GPS measurements in order to correct inertial outputs as done in figure 7. This may be done in an open loop manner or in a closed loop manner.
The dynamical evolution of the system is given by inertial error model equations. The measurement vector consists of the difference between two PRs to each satellite (GPS PR and predicted PR computed with inertial data).

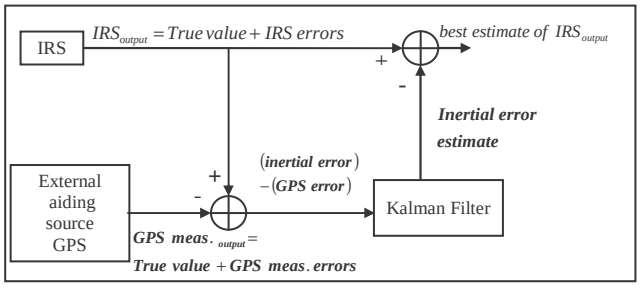

Figure 7. Open loop GPS/IRS hybridization

Filter error state model

Each component δx of the Kalman filter state vector stands for the difference between the true value x and the measured $\tilde{x}$ (or computed $\hat{x}$) value.
The state vector consists of a 17 error state variables

$$\Delta\mathbf{X} = [\boldsymbol{\rho}, \boldsymbol{\delta v}, \boldsymbol{\delta p}, \boldsymbol{\delta\omega}, \boldsymbol{\delta f}, \boldsymbol{\delta b}]^T$$

where

$\boldsymbol{\rho}$	***Attitude error vector***
$\delta\varphi \quad (\varepsilon_N)$	roll error
$\delta\theta \quad (\varepsilon_E)$	pitch error
$\delta\psi \quad (\varepsilon_D)$	yaw error

$\boldsymbol{\delta v}$	***Inertial velocity error vector***
δv_N	north velocity error
δv_E	east velocity error
δv_D	vertical velocity error
$\boldsymbol{\delta r}$	***Inertial position error***
δL	latitude error
δG	longitude error
δh	altitude error
$\boldsymbol{\delta\omega}$	***Gyro drift*** $m-$***frame***
$\delta\omega_x$	x-axis gyro drift (m)
$\delta\omega_y$	y-axis gyro drift (m)
$\delta\omega_z$	z-axis gyro drift (m)
$\boldsymbol{\delta f}$	***Accelero bias*** $m-$***frame***
δf_x	x-axis accelero bias (m)
δf_y	y-axis accelero bias (m)
δf_z	z-axis accelero bias (m)
$\boldsymbol{\delta b}$	***Receiver clock error vector***
b	receiver clock bias
$\dot{b}$	receiver clock bias drift

Table 1. Kalman filter state vector.

Many different inertial error models are available in literature. They are actually equivalent [5]. In our system the inertial navigation error model applied is

$$\begin{aligned}\dot{\boldsymbol{\rho}} &= \boldsymbol{\delta\omega} + \boldsymbol{\omega}^{\mathbf{n}}_{\mathbf{In}} \times \boldsymbol{\rho} \\ \dot{\boldsymbol{\delta v}} &= \boldsymbol{\delta f} + \left(\boldsymbol{\omega}^{\mathbf{n}}_{\mathbf{Ie}} + \boldsymbol{\omega}^{\mathbf{n}}_{\mathbf{In}}\right) \times \boldsymbol{\delta v} + \boldsymbol{\rho} \times \mathbf{a}^{\mathbf{n}}_{\mathbf{mI}} \\ \dot{\boldsymbol{\delta r}} &= \boldsymbol{\delta v} + \boldsymbol{\omega}^{\mathbf{n}}_{\mathbf{en}} \times \boldsymbol{\delta r}\end{aligned} \qquad (1)$$

Using inertial data as nominal trajectory these non-linear equation are linearized and lead to the matrix presentation of the dynamical evolution equation of the linearized Kalman filter [6]:

$$\dot{\mathbf{X}} = \mathbf{F} \cdot \mathbf{X} + \mathbf{v} \qquad (2)$$

where $\mathbf{F}$ is the state transition matrix

$$\mathbf{F} = \begin{bmatrix} \mathbf{F}_{\rho\rho} & \mathbf{F}_{\rho v} & \mathbf{F}_{\rho r} & \mathbf{F}_{\rho\omega} & 0 & 0 & 0 \\ \mathbf{F}_{v\rho} & \mathbf{F}_{vv} & \mathbf{F}_{vr} & 0 & \mathbf{F}_{vf} & 0 & 0 \\ \mathbf{F}_{r\rho} & \mathbf{F}_{rv} & \mathbf{F}_{rr} & 0 & 0 & 0 & 0 \\ 0 & 0 & 0 & \mathbf{F}_{\omega\omega} & 0 & 0 & 0 \\ 0 & 0 & 0 & 0 & \mathbf{F}_{ff} & 0 & 0 \\ 0 & 0 & 0 & 0 & 0 & 0 & 1 \\ 0 & 0 & 0 & 0 & 0 & 0 & 0 \end{bmatrix} \qquad (3)$$

and the noise state vector w is a zero-mean Gaussian white noise vector, whose components are all independent.
Let Φ be the discret form of $\mathbf{F}$.

Let be Q the state noise covariance matrix:

$$\mathbf{Q} = E\left[\mathbf{v} \cdot \mathbf{v}^T\right] \qquad (4)$$

Filter error measurement model

Each component of the measurement vector $\mathbf{z}$ at filter's input is the difference between two PRs to each satellite. One is the measured PR input from the GPS receiver; the other is the predicted PR computed on the basis of the satellite positions obtained from the GPS receiver and the user location as calculated by the IRS.
The coefficients of the measurement matrix $\mathbf{H}$ are direction cosine computed from the GPS navigation equation linearization.
Let $\mathbf{R}$ be the measurement noise covariance matrix: all measurement noises are independent.

The size of the $\mathbf{z}-$vector and the $\mathbf{R}$ and $\mathbf{H}-$matrices depend on the number of tracked satellite.

Kalman filters implementation

Let ij be the subscript for the Kalman filter F_{ij}. The maximum number of tracked satellites is $N = 10$.
There is one primary filter, N sub-filters, and N*(N-1) sub-sub-filters that are running in parallel.
The estimated state vector for each are

primary filter: $\boldsymbol{\Delta\hat{x}}_{\mathbf{00}}$

sub-filter: $\boldsymbol{\Delta\hat{x}}_{\mathbf{0n}}$, $n = 1, N$

sub-sub-filter: $\boldsymbol{\Delta\hat{x}}_{\mathbf{nm}}$, $n = 1, n; m = 1, N; m \neq n$

The estimation error covariance matrix for each is

primary filter: $\mathbf{P}_{\mathbf{00}}$

sub-filter: $\mathbf{P}_{\mathbf{0n}}$, $n = 1, N$

sub-sub-filter: $\mathbf{P}_{\mathbf{nm}}$, $n = 1, n; m = 1, N; m \neq n$

where

$$\mathbf{P}_{\mathbf{ij}} = E\left[\boldsymbol{\delta x}_{\mathbf{ij}} \cdot \boldsymbol{\delta x}_{\mathbf{ij}}{}^T\right], \quad \boldsymbol{\delta x}_{\mathbf{ij}} = \boldsymbol{\Delta\hat{x}}_{\mathbf{ij}} - \boldsymbol{\Delta x}$$

Δx is the true error between estimated IRS and true position: $\Delta x = \hat{X}_{IRS} - X$

The Kalman Gain matrix for each is

primary filter: $\mathbf{K_{00}}$

sub-filter: $\mathbf{K_{0n}}$, $n=1,N$

sub-sub-filter: $\mathbf{K_{nm}}$, $n=1,n;m=1,N;m\neq n$

Because GPS and IRS data are not available at the same rate, the error model is updated at $100Hz$ and Kalman filters measurements are updated at $1Hz$.
So the Kalman corrections are available every second.

Next section details implementation of FDE algorithm.

FAULT DETECTION AND HORIZONTAL PROTECTION LEVEL

Fault detection is performed by estimating the separation between the primary filter estimate and each of the N sub-filters estimates in the horizontal plane.

At each estimation time the discriminator for the n[th] sub-filter is based on Solution Separation vector between the primary filter and the n[th] sub-filter:

$$\begin{aligned}\mathbf{dx_{0n}}^{+}(k) &= \Delta\hat{\mathbf{x}}_{\mathbf{00}}{}^{+}(k)-\Delta\hat{\mathbf{x}}_{\mathbf{0n}}{}^{+}(k)\\ &=\boldsymbol{\delta}\mathbf{x}_{\mathbf{00}}{}^{+}(k)-\boldsymbol{\delta}\mathbf{x}_{\mathbf{0n}}{}^{+}(k),\ n=1\ldots N\end{aligned} \quad (5)$$

whose statistics are described by the covariance matrix

$$\mathbf{dP_{0n}}^{+}(k)=E\left[\left(\mathbf{dx_{0n}}^{+}(k)\right)\cdot\left(\mathbf{dx_{0n}}^{+}(k)\right)^{T}\right] \quad (6)$$

Since $\mathbf{dx_{0n}}$ and $\boldsymbol{\delta}\mathbf{x_{00}}$ are statically dependent, let us form the 34x1 error vector

$$\boldsymbol{\delta}\mathbf{x}^{+}(k)=\left[\boldsymbol{\delta}\mathbf{x_{00}}{}^{+}(k),\Delta\mathbf{x_{0n}}{}^{+}(k)\right]^{T} \quad (7)$$

whose statistics are described by

$$\begin{aligned}\mathbf{dP_{0n}}^{\mathbf{dual}+}(k) &= E\left[\left(\boldsymbol{\delta}\mathbf{x}^{+}(k)\right)\cdot\left(\boldsymbol{\delta}\mathbf{x}^{+}(k)\right)^{T}\right]\\ &=\begin{bmatrix}\mathbf{P_{00}}^{+}(k) & \mathbf{cross\,corr.}\\ \mathbf{cross\,corr.} & \mathbf{dP_{0n}}^{+}(k)\end{bmatrix}\end{aligned} \quad (8)$$

Given the fact that

$$\begin{aligned}\mathbf{dx_{0n}}^{+}(k) &= \Delta\hat{\mathbf{x}}_{\mathbf{00}}{}^{+}(k)-\Delta\hat{\mathbf{x}}_{\mathbf{0n}}{}^{+}(k)\\ &=\boldsymbol{\delta}\hat{\mathbf{x}}_{\mathbf{00}}{}^{+}(k)-\Delta\hat{\mathbf{x}}_{\mathbf{0n}}{}^{+}(k)+\Delta\mathbf{x}\end{aligned} \quad (9)$$

and

$$\boldsymbol{\delta}\mathbf{x}^{-}(k)=\underbrace{\begin{bmatrix}\boldsymbol{\Phi} & 0\\ 0 & \boldsymbol{\Phi}\end{bmatrix}}_{\Pi}\cdot\boldsymbol{\delta}\mathbf{x}^{+}(k-1)+\begin{bmatrix}\mathbf{v}\\ 0\end{bmatrix} \quad (10)$$

one can show that

$$\mathbf{dP_{0n}}^{\mathbf{dual}+}(k)=\boldsymbol{\Sigma}\cdot\mathbf{dP_{0n}}^{\mathbf{dual}-}(k)\cdot\boldsymbol{\Sigma}^{T}+\boldsymbol{\Gamma}\cdot\mathbf{R}\cdot\boldsymbol{\Gamma}^{T} \quad (11)$$

with

$$\boldsymbol{\Sigma}=\begin{bmatrix}I-\mathbf{K_{00}}\cdot\mathbf{H_{00}} & 0\\ \left(\mathbf{K'_{0n}}-\mathbf{K_{00}}\right)\cdot\mathbf{H_{00}} & I-\mathbf{K'_{0n}}\cdot\mathbf{H_{00}}\end{bmatrix} \quad (12)$$

$$\Gamma=\begin{bmatrix}\mathbf{K_{00}}\\ \mathbf{K_{00}}-\mathbf{K'_{0n}}\end{bmatrix} \quad (13)$$

$$\boldsymbol{\delta}\mathbf{P_{0n}}^{\mathbf{dual}-}(k)=\boldsymbol{\Pi}\cdot\boldsymbol{\delta}\mathbf{P_{0n}}^{\mathbf{dual}+}(k-1)\cdot\boldsymbol{\Pi}^{T}+\begin{bmatrix}\mathbf{Q} & 0\\ 0 & 0\end{bmatrix} \quad (14)$$

$\mathbf{K'_{0n}}$ is constructed from $\mathbf{K_{0n}}$ so that it operates on the full set of measurements by extending the 17x(N-1) matrix $\mathbf{K_{0n}}$ sub-solution matrix with a n[th] zeroed column.

Detection threshold D_{0n} vs. test statistics d_{0n}

The statistic of the horizontal separation vector $\mathbf{X_H}=\mathbf{dx_{0n}}^{+}[\mathbf{7:8}]$, is described by $\mathbf{L_{0n}}=\mathbf{dP_{0n}}^{+}[\mathbf{7:8,7:8}]$. Because separations on North and East axes are correlated, $\mathbf{L_{0n}}$ is projected in an orthogonal plane so that,

$$\mathbf{L_{0n}}=\mathbf{P_{\perp}}\cdot\boldsymbol{\Delta}\cdot\mathbf{P_{\perp}}^{\mathbf{T}} \quad (15)$$

and $\mathbf{X_{\perp}}=\mathbf{P_{\perp}}^{T}\cdot\mathbf{X_H}$ is a Gaussian vector whose covariance matrix is the diagonal matrix $\boldsymbol{\Delta}$ (eigenvalues matrix of $\mathbf{L_{0n}}$).

One of the two eigenvalues is dominating. Let λ^{dP} be the approximate variance ($\Delta(1,1)$ *or* $\Delta(2,2)$) of the error in the horizontal plane.

For each sub-filter the decision threshold is set so that d_{0n} will exceed D_{0n} with the probability P_{FA}. Since all sub-filters have the same chance of false alarm

$$D_{0n} = \sqrt{\lambda^{dP}} \cdot Q^{-1}\left(\frac{P_{FA}}{2N}\right) \text{ with } Q^{-1}(u) = erfc(u)$$

and $d_{0n} = |X_{\perp}(1)| \text{ or } |X_{\perp}(2)|$ (16)

depending on $\lambda^{dP} = \Delta(1,1) \text{ or } \lambda^{dP} = \Delta(2,2)$

The test for detecting one failure satellite is

H_0 no detection: $d_{0n} \le D_{0n}$

H_1 detection: $d_{0n} > D_{0n}$ for at least one $n, n = 1, N$

Horizontal protection level HPL

By definition the HPL is the error bound that contains the primary filter error with a probability of $1 - p_{MD}$ when $d_{0n} = D_{0n}$.

Since for each sub-filter

$\delta\mathbf{x_{00}}^{+}(k) = \mathbf{dx_{0n}}^{+}(k) + \delta\mathbf{x_{0n}}^{+}(k), n = 1 \ldots N$ (17)

at detection (for the n[th] subset)

$$HPL_n = D_{0n} + a_{0n} \quad (18)$$

where a_{0n} is an upper bound of the n[th] sub-filter horizontal error $\Delta\mathbf{x_{0n}}^{+}[\mathbf{7:8}]$ whose distribution is described by $\mathbf{L} = \mathbf{P_{0n}}^{+}[\mathbf{7:8,7:8}]$.

Let $\lambda^{P_{0n}}$ be the maximum eigenvalue of $\mathbf{L}$

$$a_{0n} = \sqrt{\lambda^{P_{0n}}} \cdot Q^{-1}(1 - p_{MD}) \quad (19)$$

Besides we have to consider the rare normal performance that is to say the contribution of the primary filter HPL_0

$$HPL_0 = \sqrt{\lambda^{P_{00}}} \cdot Q^{-1}\left(\frac{P_{ff}}{2}\right) \quad (20)$$

where P_{ff} is the rare normal performance rate and $\lambda^{P_{00}}$ the maximum eigenvalue of $\mathbf{P_{00}}^{+}[\mathbf{7:8,7:8}]$.

The horizontal protection level is

$$HPL = \max\{HPL_0, \max(HPL_n)\}, n = 1, N \quad (21)$$

FAULT EXCLUSION AND HORIZONTAL EXCLUSION LEVEL

Fault exclusion is accomplished in the same manner than detection but one layer down in the filters hierarchy.

The discriminator of each of the sub-sub-filter is the separation between each sub-sub-filter estimate solution and its parent's sub-filter estimate solution in the horizontal plane. For the n[th] sub-filter they are

$$\mathbf{dx_{nm}}^{+}(k) = \Delta\hat{\mathbf{x}}_{\mathbf{0n}}^{+}(k) - \Delta\hat{\mathbf{x}}_{\mathbf{nm}}^{+}(k) = \delta\mathbf{x_{0n}}^{+}(k) - \delta\mathbf{x_{nm}}^{+}(k), \quad m = 1 \ldots N, m \ne n \quad (22)$$

whose statistics are described by the covariance matrix

$$\mathbf{dP_{nm}}^{+}(k) = E\left[\left(\mathbf{dx_{nm}}^{+}(k)\right) \cdot \left(\mathbf{dx_{nm}}^{+}(k)\right)^{T}\right] = E\left[\left(\delta x_{\mathbf{0n}}^{+}(k) - \delta x_{\mathbf{nm}}^{+}(k)\right)\left(\delta x_{\mathbf{0n}}^{+}(k) - \delta x_{\mathbf{nm}}^{+}(k)\right)^{T}\right] = \mathbf{P_{0n}}^{+}(k) - \mathbf{P_{nm}^{cross+}}(k) - \left(\mathbf{P_{nm}^{cross+}}(k)\right)^{T} + \mathbf{P_{nm}}^{+}(k) \quad (23)$$

Exclusion threshold D_{nm} vs test statistics d_{nm}

For each sub-sub-filter the decision threshold is set so that (assuming that each filter F_{nm} has the same chance for a false alarm)

$$D_{nm} = \sqrt{\lambda^{dP_{nm}}} \cdot Q^{-1}\left(\frac{P_{FA}}{2(N-1)}\right) \quad (24)$$

where $\lambda^{dP_{nm}}$ the maximum eigenvalue of $\mathbf{L_{nm}} = \mathbf{P_{nm}}^{+}[\mathbf{7:8,7:8}]$

The test statistic associated to D_{nm} is

$$d_{nm} = |X_{m\perp}(1)| \text{ or } |X_{m\perp}(2)| \quad (25)$$

where $\mathbf{X}_{m\perp} = \mathbf{P}_{m\perp}^{T} \cdot \mathbf{dx_{nm}}^{+}[\mathbf{7:8}]$

with $\mathbf{L_{nm}} = \mathbf{P_{m\perp}} \cdot \mathbf{\Delta} \cdot \mathbf{P_{m\perp}}^{\mathbf{T}}$

Satellite r is excluded as the failed satellite if and only if

$d_{rm} < D_{rm}$ for all $m \ne r$

and

$d_{nm} \ge D_{nm}$ for at least one $m \ne n$ for all $n \ne r$

Horizontal exclusion level HEL

By definition HEL is the error bound that contains the primary filter error with a probability of $1 - p_{FE}$ when the failure is excluded.

"For a failed exclusion to occur, the solution of one of the sub-filters $\Delta\hat{\mathbf{x}}_{\mathbf{0n}}$ which does contain the failed satellite must be separated from one of its sub-sub-filter's

solution $\Delta\hat{\mathbf{x}}_{\mathbf{nm}}$ by less than the threshold D_{nm} plus the sub-sub-filter position error" [2]

Let a_{nm} be the sub-sub-filter horizontal estimation error bound and $\lambda^{P_{nm}}$ be the maximum eigenvalue of $\mathbf{P}_{nm}{}^{+}[\mathbf{7:8,7:8}]$

$$a_{nm} = \sqrt{\lambda^{P_{nm}}} \cdot Q^{-1}(1 - p_{FE}) \qquad (26)$$

For the nth sub-filter HEL_n is given by

$$HEL_n = \max\{D_{nm} + a_{nm}\}, m = 1, N \qquad (27)$$

And the horizontal exclusion level is

$$HEL = \max\{HEL_n\}, n = 1, N \qquad (28)$$

RESULTS OF SIMULATIONS

The whole system has been implemented in Matlab language. This section presents the firsts results obtained in testing the FDE algorithm for detection and isolation of failures causing slowly increasing ramp error.

Conditions for the simulation

GPS constellation

- Mask angle 5° (10 SVs, no constellation change)

GPS receiver

- Total receiver noise 12.5m (1σ)
- Correlated noise: 1srt order Markov process ($\tau = 15\min, \sigma = 4.8m$)

Inertial error sources

Error source (one sigma)	*Good*	*Low cost*
Gyro constant bias: °/hr	0.01	1
Gyro white noise: °s/ $\sqrt{Hz}$	3.10^{-5}	0.001
Accelero constant bias: µg	50	500
Accel. white noise: µg/ $\sqrt{Hz}$	6.4	64

Table 2. Good / low cost IRS error sources

GPS/IRS hybridization is performed in an open-loop manner for good IRS, and closed and open loop manner for low cost IRS.

FDE algorithm

- No. of independent tests/hr=4
- $P_{FA} = 1/3.10^{-6}/hr = 1/12.10^{-6}/test$
- $P_{ff} = 1/3.10^{-8}/test$
- ramp error size (m/s) (time 400s)
  $0.1, 0.2, 0.5, 1, 2, 5$
  on the worst case satellite (SV 4).

Trajectory: duration 600s

- The simulated trajectory is an approach to Toulouse-Blagnac Airport from AGN VOR. It includes a turn at time 180s and a descent at time 280 s.

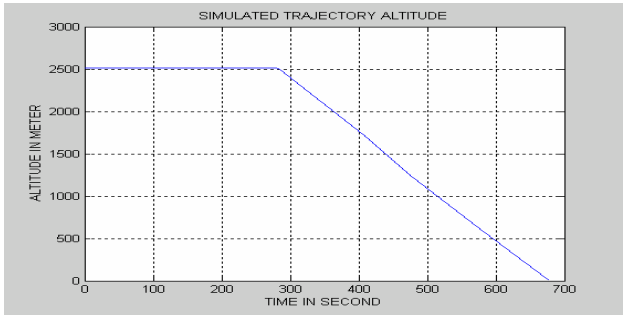

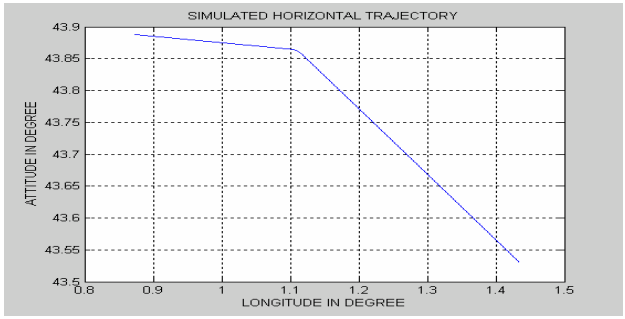

Figure 8.Simulated trajectory

- During the turn, heading angle is varying from 098° to 145°. Roll angle is varying with a rate of 1 (180°/60s). Pitch angle is also varying since the aircraft is supposed to keep its altitude.
- During the descent only pitch angle is varying according trajectory slope.

Results

Figure 9 shows Horizontal Protection Level for RAIM and AAIM (HPL), and Horizontal Exclusion Level for AAIM (HEL) using Solution Separation algorithm.

AAIM HPL and HEL convergence occurs after 250s of simulation. HPL and HEL are much smaller (under 30m) than RAIM HPL (70m). AAIM HEL is greater than HPL by approximately 5m. AAIM HPL and HEL obtained using closed loop are the same than those obtained using open loop.

Figure 10 shows how detection is achieved on channel 4 in presence of a failure when GPS measurement noise is only due to white-Gaussian noise. Before the failure occurs at 400s the discriminator is zero-mean and is lower than the decision threshold. The failure detection occurs

when the discriminator exceeds the decision threshold. The IRS quality seems to have an influence: HPL and HPE obtained hybridizing GPS with a good IRS are in the order of 10m under those obtained hybridizing GPS with a low cost IRS. But no extensive Monte-Carlo simulation has been performed.

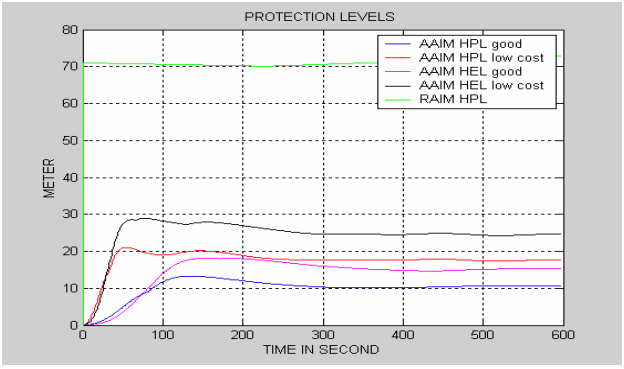

Figure 9. Horizontal protection levels.

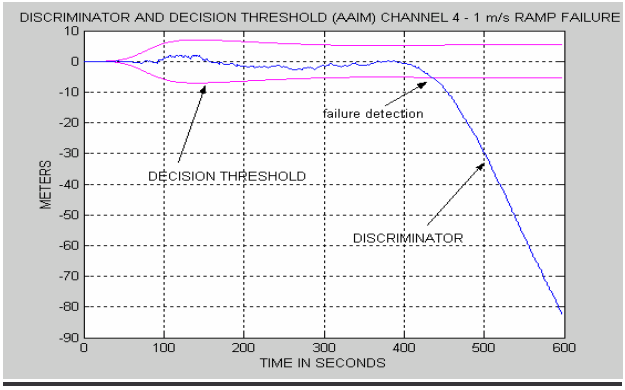

Figure 10. Discriminator deviation due satellite failure causing ramp

The following tables show examples of detection and exclusion performance with only white measurement noise.
In these examples, AAIM algorithm is detecting satellite failure earlier than RAIM algorithm and the delay between detection and isolation doesn't exceed 20 s (table 3). Besides, for all the simulations the faulty satellite was detected and isolated before the horizontal error grows over around 13m (table 4, 5).
In the case of open-loop, the low cost IRS drifts tend to make the whole system derivate. In the case of closed loop bad estimates of inertial errors due to ramp failure tend to miss-calibrate the inertial platform. Thus position error drift is not only due to satellite failure but also inertial drift. In these cases detection occurs earlier, these results might yield us to think that the false alarm rate could increase.

Failure introduced at 400s	RAIM	AAIM		
		open loop		closed
		good	Low cost IRS	
Ramp: 0.1(m/s)				
detection	> 600s	566 s	594s	> 600s
SV4 isolation	no simu.	586 s	> 600s	> 600s
Ramp: 0.5 (m/s)				
Detection	565 s	451 s	439s	443s
SV4 isolation	no simu.	458 s	445s	446s
Ramp: 1 (m/s)				
Detection	500 s	435 s	433s	428s
SV4 isolation	no simu.	439 s	435s	432s
Ramp: 5 (m/s)				
Detection	415	411 s	412s	411s
SV4 isolation	no simu.	413 s	413s	412s

Table 3. RAIM and AAIM times of detection and isolation.

Ramp size	RAIM	AAIM		
		Open loop		closed
		good	Low cost IRS	
0.1(m/s)	>7.1 m	5.2m	9.5m	> 6m
0.5 (m/s)	34.1m	5.3m	7m	5.3m
1 (m/s)	32.5m	5.7m	12m	10.5 m
5 (m/s)	8.5m	5.8m	10.6m	9 m

Table 4. Error size at detection time in the horizontal plane (good IRS)

Ramp size	AAIM		
	Open loop		closed
	good IRS	Low cost IRS	
0.1(m/s)	6.1m	> 9.5m	> 6m
0.5 (m/s)	6.5m	9.5m	5.8m
1 (m/s)	7m	13m	11.2 m
5 (m/s)	7.2m	12.5m	10.5 m

Table 5. Error size at AAIM isolation time in the horizontal plane (good IRS)

One main advantage of this algorithm is that it is able to detect any type of failures. But it may become a drawback if the process is bad modelled in the Kalman filter. Simulations were made assuming the measurement noise was not only white noise. Many false detections (only due to measurement noise) and false isolations were observed. Indeed in that case correlated noise was interpreted by the FDE algorithm as a failure.
Figure 11 and 12 show AAIM HPL with only white measurement noise generated and mixed measurement noise. In the simulation context of figure 12, results show a false detection alert at time $404s$ whereas the ramp error on measurement is not large enough to be detected in the case illustrated in figure 10. In fact, in figure 12,

correlated noises make the GPS measurement look like being affected by ramp failure which is certainly the reason of this alert. Figure 13 shows the miss-modelling impact on the discriminator computed for sub-filter F_{04} that is no more a zero-mean variable due to correlated noise addition on range measurement. On figure 10 the discriminator deviation is only due to satellite failure causing a ramp.

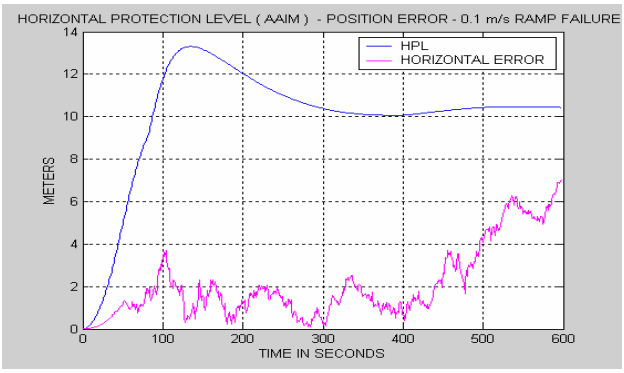

Figure 11. White noise measurement noise observation

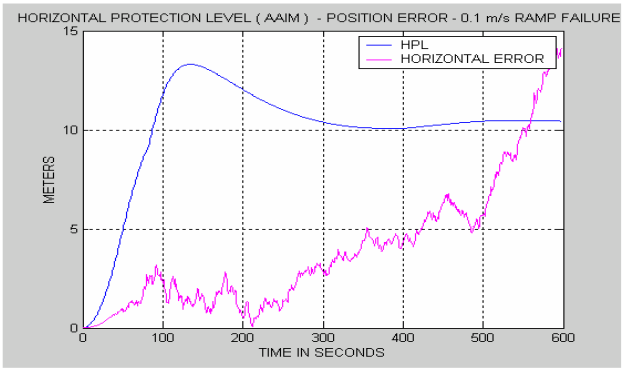

Figure 12. White + correlated noise measurement observation

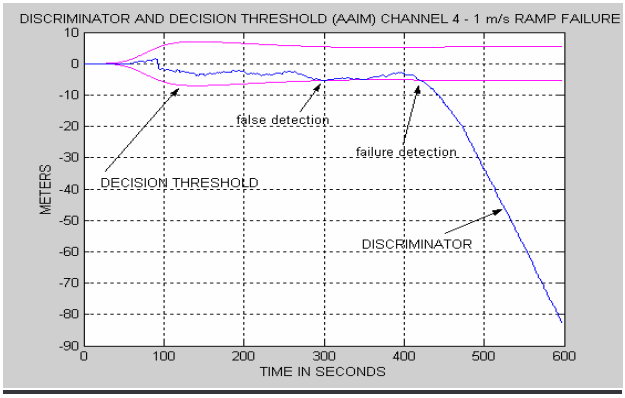

Figure 13. Discriminator deviation due to correlated noise

Solution to take into account the correlated noise on GPS measurement is to estimate the evolution of this process. The Kalman filters state vector is extended by adding as many states as the number of tracked satellites. The i^{th} supplemental state stands for GPS range bias error for i^{th} satellite.

CONCLUSION

Solution Separation method is a very appealing Fault detection and Exclusion algorithm because of its rigorousness. This paper presents an open-loop GPS/IMU system being investigated by the ENAC in order to start appreciating the Solution Separation algorithm ability of fault isolation. Simulations were performed assuming NPA requirements and satellite failure causing a ramp from 0.1m/s to 5m/s. AAIM HPL and HEL are the order of 20-30 m and are lower than RAIM HPL (closed to 70m). Isolation of the faulty satellite occurs less than 20 seconds after fault detection arise. Low cost IRS is affected by inertial drift that pollutes the hybridized solution causing false alarm in open-loop hybridization. Finally the whole FDE algorithm performance seems to greatly depend on Kalman filter miss-modelization. Thus implementation improvements have to be taken account such as the correlation measurement noise in the Kalman filter model and will be the issue of further works.

REFERENCES

1. - M. BRENNER, Integrated GPS/inertial detection availability, Journal of The Institute of Navigation, Sept. 1995.
2 - K. VANDERWERF, FDE Using Multiple Integrated GPS/Inertial Kalman Filters in the Presence of Temporally and Spatially Correlated Ionospheric Errors, ION GPS 2001, 11-14 Sept. 2001, Salt Lake City
3. -Requirements and Test Procedures for Tightly Integrated GPS/Inertial Systems Appendix R to DO-229C,.
4.- J. C. RADIX, Systèmes Inertiels à Composants Liés “Strapdown”, Cépadues Educs, 1991.
5.- R. DA, Investigation of a Low-Cost and High-Accuracy GPS/IMU System, Proceedings of ION GPS, Sept. 1996.
6.- FARRELL J. A., BARTH M., The Global Positionning System & Inertial navigation, McGraw-Hill, 1998.